Janus Superiority of Membranes in Chemical Engineering and Beyond

Hao-Cheng Yang,[+*[a,b]] Yi-Zhou Chen,[+[a]] Kai Li,[[a,b]] Xin-Yu Guo,[[a]] Qi-Rui Jiang,[[a]] Seth B. Darling,*[[c,d]] Zhi-Kang Xu*[[a,b]]

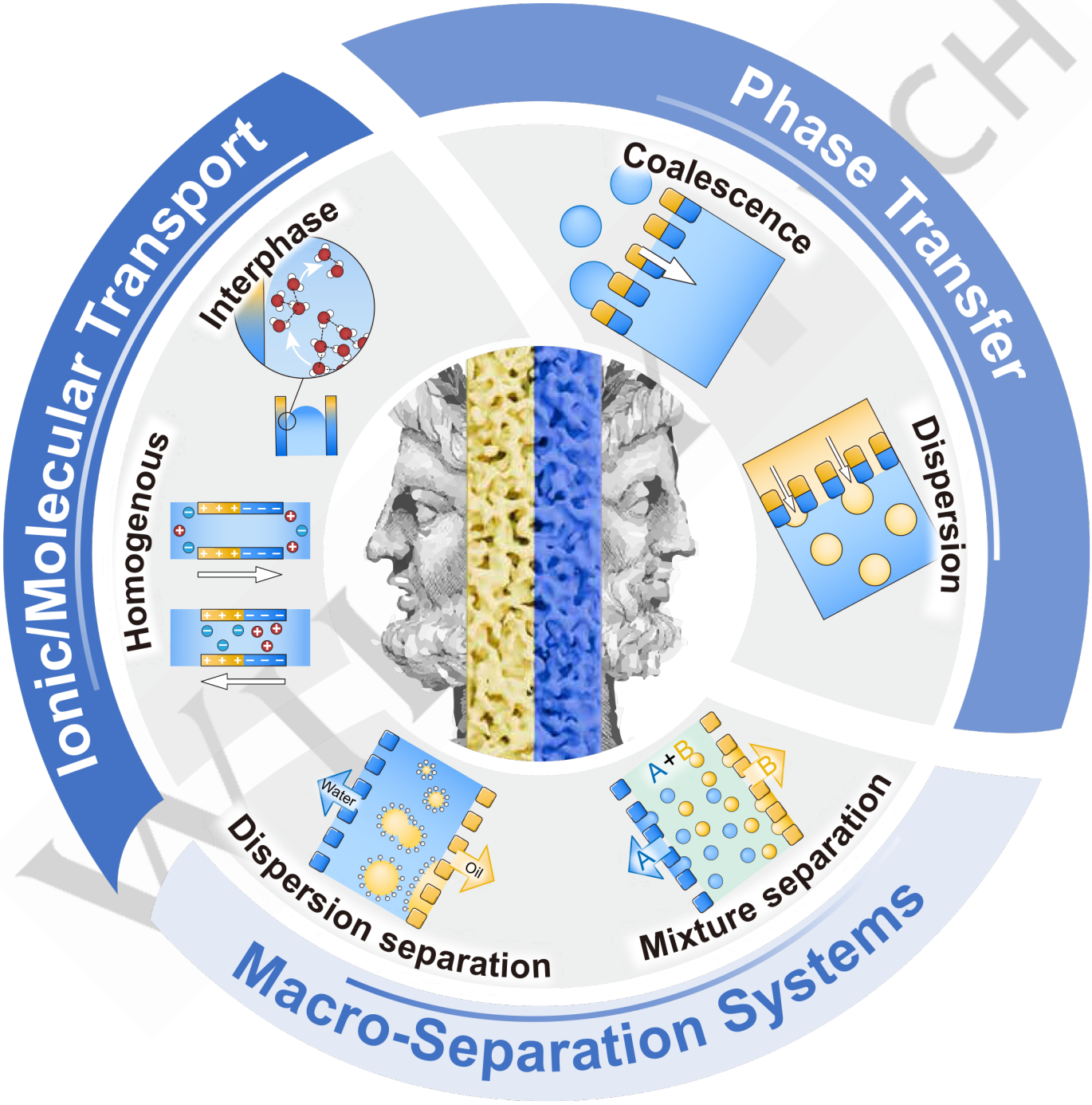

[a] Prof. H.-C Yang, Y.-Z Chen, K. Li, X.-Y Guo, Q.-R. Jiang, Prof. Z.-K. Xu
MOE Engineering Research Center of Membrane and Water Treatment Technology, and Key Lab of Adsorption and Separation Materials & Technologies of Zhejiang Province, Department of Polymer Science and Engineering
Zhejiang University
Hangzhou 310058, P.R. China.
E-mail: yanghch@zju.edu.cn (H.-C. Yang), xuzk@zju.edu.cn (Z.-K. Xu).

[b] Prof. H.-C Yang, K. Li, Prof. Z.-K. Xu
The "Belt and Road" Sino-Portugal Joint Lab on Advanced Materials, International Research Center for X Polymers
Zhejiang University
Hangzhou 310058, P.R. China.

[c] Dr. S.B Darling
Center for Molecular Engineering, Chemical Sciences and Engineering Division and Advanced Materials for Energy-Water Systems (AMEWS) Energy Frontier Research Center
Argonne National Laboratory
Lemont, IL 60439, USA
E-mail: darling@anl.gov (S.B. Darling).

[d] Dr. S.B Darling
Pritzker School of Molecular Engineering
University of Chicago
Chicago, IL 60637, USA

[+] The authors contribute equally to this work.

Biography: Hao-Cheng Yang is a ZJU-100 Young Professor at Zhejiang University. He received his Ph.D. in Polymer Science from Zhejiang University in 2017, followed by postdoctoral research at Argonne National Laboratory. He joined Sun Yat-sen University as an Associate Professor in 2018 and moved to Zhejiang University in 2023. His research focuses on the development of advanced membrane materials (e.g. Janus membranes) and separation processes, with more than 100 papers on these topics.

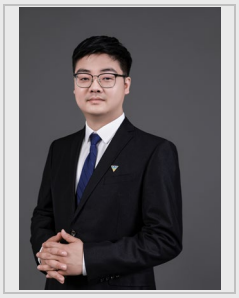

Biography: Seth Darling is Chief Science & Technology Officer of Advanced Energy Technologies and a Senior Scientist at Argonne National Laboratory. He directs the Advanced Materials for Energy-Water Systems (AMEWS) EFRC and is a Senior Scientist at the Pritzker School of Molecular Engineering at the University of Chicago. His research focuses on molecular engineering and advanced materials for water purification. He has published over 150 papers, authored two books, holds more than 20 patents, and lectures widely on energy and water topics.

Biography: Prof. Zhi-Kang Xu is a Qiushi Distinguished Professor at Zhejiang University. He received his Ph.D. degree in polymer chemistry and physics at Zhejiang University in 1991. The principal research efforts of his group focus on polymer membranes with surface and interface engineering for sustainable applications. He has published more than 400 papers with over 24000 citations.

Abstract: Janus configurations, characterized by their inherent asymmetry, enable directional mass transfer in membrane materials that drives novel and energy-efficient chemical processes. This Janus superiority spans applications from nanoscale molecular and ionic transport to macro-scale separation systems with asymmetric spatial architectures. This review provides an analysis of the material foundations including design principles, structure regulation, and scalability challenges underlying Janus membranes. We explore the physics that govern their unique behavior and examine their diverse applications across chemical engineering, including phase transfer, and molecular or ionic transport. Through a multiscale perspective, we provide a comprehensive understanding of the impact of Janus superiority in advancing chemical engineering technologies. Finally, we discuss the hurdles in translating theoretical advances into practical applications and propose promising avenues for future research to harness the full potential of Janus membranes and systems in addressing global challenges related to energy, sustainability, and beyond.

1. The Advent of Janus Membranes

The development of energy-efficient processes is essential for achieving carbon emission reduction targets to address the urgent challenge of climate change, while also conserving energy to meet the growing demand from emerging sectors such as advanced manufacturing, artificial intelligence, blockchain, and cloud computing. Separation processes are notably energy-intensive within industrial sectors, accounting for 44%-55% of total energy consumption.[1] Traditional processes like distillation and crystallization necessitate substantial energy due to phase transitions. In contrast, membrane separation offers a promising solution by significantly reducing energy consumption.[2] This technique, widely applied in industries like petrochemicals, environment remediation, and seawater desalination, does not involve phase transitions and thus demands significantly less energy[3–5] While pursuing the ultimate separation performance of membrane materials, there is a growing focus on approaching the theoretical limit of separation energy consumption. Typically, membrane separation relies on directional mass transfer driven by differences in chemical potentials—such as pressure, electric potential, or temperature—across the membrane, which can be termed an "external driving force". Since the separation process inherently reduces entropy, boosting mass transfer in the desired direction while resisting it in the opposite direction proves advantageous. When mass transfer in opposing directions differs due to specific membrane properties or structures, such properties or structures could be considered as an “internal driving force”. Janus membrane appears as a typical material exhibiting this “internal driving force”.[6]

The term "Janus membrane" appeared around 2014, initially referring to porous membranes with one side being hydrophobic and the other side being hydrophilic.[7] However, considering the feature of unidirectional transport, the earliest instance can be traced back to the Janus fabrics reported by Lin’s group in 2010.[8] Over time, the concept of Janus membranes was expanded to include membranes with asymmetric structures, compositions, or properties. Nevertheless, traditional separation membranes fabricated through phase inversion and interfacial polymerization often also exhibit asymmetric pore structures or compositions. To distinguish Janus membranes from traditional asymmetric membranes, our group proposed a more rigorous definition: Janus membranes possess opposite properties on both sides,[9] such as hydrophilicity-hydrophobicity or positive-negative charges. This definition aligns closely with the original concept of Janus materials originally proposed by P. G. de Gennes, the Nobel laureate in physics in 1991, and has since been widely accepted in the field.[10]

Among Janus membranes, those with asymmetric wettability, such as hydrophilic-hydrophobic combinations, are the most prevalent. Early studies highlighted their unique liquid directional transfer capabilities, where water droplets could pass from the hydrophobic side to the hydrophilic side, but not the reverse. Despite their intriguing behavior, Janus membranes remained underexplored until around 2014, when they, along with Janus fabrics, began demonstrating unique potential in chemical engineering applications, including aeration,[11] emulsification,[12] demulsification,[13] fog harvesting,[14] membrane reactors/contactors,[15] and membrane distillation.[16] This renewed interest has since sparked rapid development in these fields (Figure 1). In subsequent years, their applications have further expanded into emerging domains such as solar evaporation,[17,18] personal thermal-moisture management,[19,20] wound dressing,[21,22] and beyond. These developments position Janus membranes as a rising star in chemical engineering, with their collective advantages encapsulated by the concept of “Janus superiority”. In a narrow sense, Janus superiority refers to the superior energy efficiency and performance of Janus membranes compared to homogeneous membranes. More broadly, it also encompasses the ability of these membranes to meet diverse functional requirements within coupled processes. In the aforementioned processes, the concept of Janus superiority is primarily manifested in phase transport. Recent studies have extended this concept to nanopores, where Janus membranes exhibit unique advantages during inter-phase molecular transport. Additionally, we have also discovered that this superiority can be applied to spatial structures constructed by membranes with opposing properties. These findings significantly broaden the potential and scope of Janus superiority across various domains.

Another category of Janus membranes with opposing surface charges appeared around 2014, which is derived from the concept of the nanofluidic diode.[23] These membranes exhibit directional ion transport behavior in

response to an applied bias, which has found applications in energy conversion and separation. It is worth noting that, from this perspective, bipolar membranes, first invented in the 1950s, also represent a subclass of Janus membranes that have been extensively investigated and practically applied.[24] Beyond, Janus separators in batteries are another category of Janus membranes, developed to suppress the “shuttle effect” in Li-S batteries.[25,26] However, these membranes typically feature asymmetric structures or components, rather than opposing properties. Similarly, some membranes labeled as "Janus" merely integrate different functions within a single membrane,[27] rather than achieving synergistic performance enhancements through opposing properties, which will not be extensively discussed here.

In this Review, we provide a comprehensive analysis of the concept of Janus superiority in membrane materials and devices, highlighting both the opportunities and challenges in this field. While previous reviews have largely focused on the fabrication techniques and applications of Janus membranes, this review aims to offer a more nuanced perspective by briefly addressing the material foundations underlying Janus superiority, including the design principles and the scalability potential of current fabrication methods. Next, we introduce the physics behind Janus superiority, providing a fundamental understanding of its mechanisms. We then explore the phenomena of Janus superiority across different scales, corresponding to diverse transport processes such as phase transfer and ionic/molecular transport, with a particular focus on its implications for membrane systems. Finally, we discuss the challenges related to the theoretical foundations, production scalability, and real-world applications of Janus membranes, while identifying the promising opportunities that Janus superiority offers for advancing chemical processes.

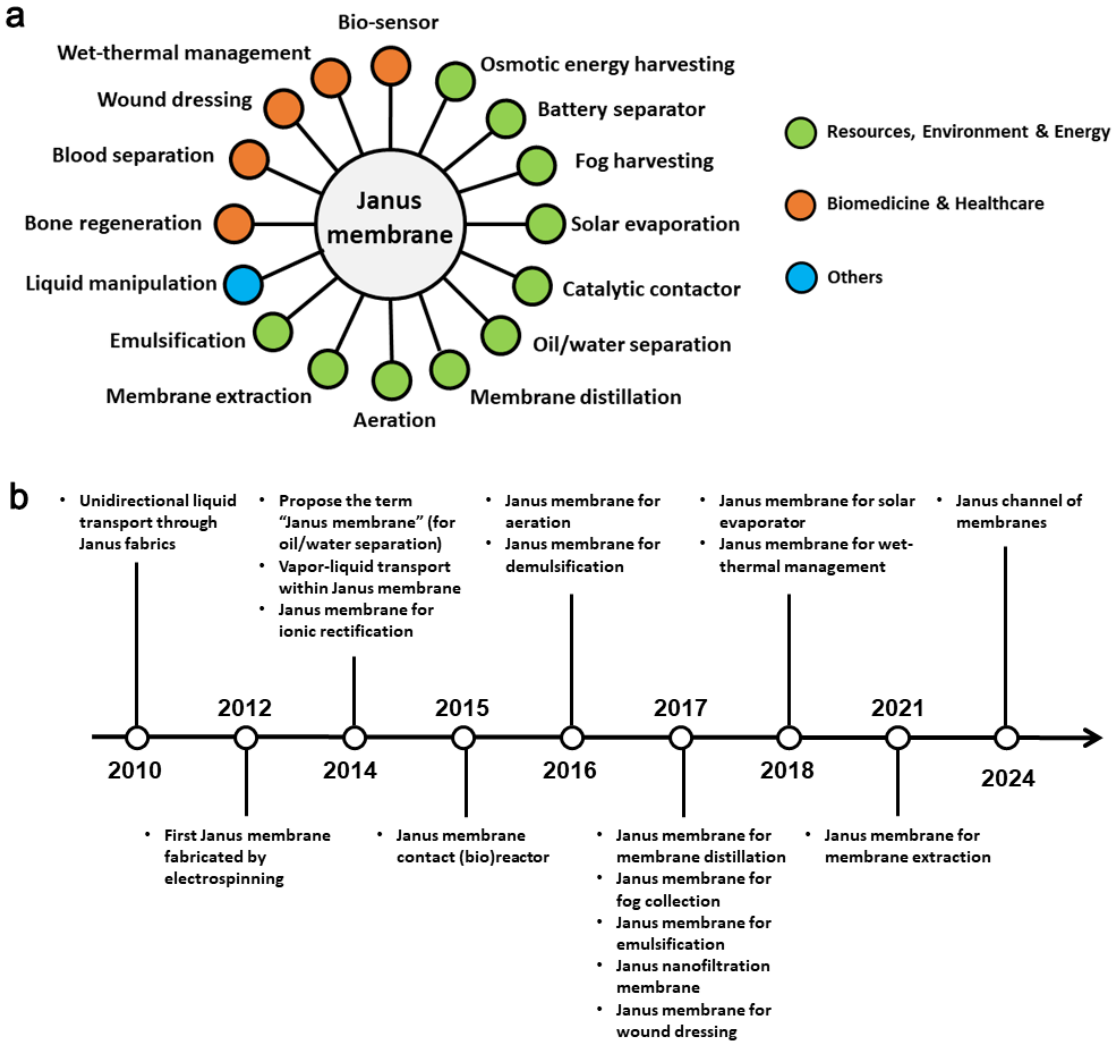

Figure 1. a. Applications of Janus membranes in chemical engineering and beyond. **b**. Milestones in the research of Janus membranes and membrane systems

2. Materials Foundations of Janus Superiority

2.1. Fabrication Principles

Janus membranes with different structures are fabricated based on distinct principles. Typically, Janus configurations can be categorized into two types: bi-layer configuration, which features a distinct boundary between the layers, and gradient configuration, which exhibits a property gradient across the membrane thickness.

From a technical perspective, Janus membranes can be constructed either by directly compositing two distinct layers or by asymmetrically modifying a uniform membrane (Figure 2a). Bi-layer Janus membranes are primarily fabricated through bi-layer compositing, though they can also be produced via interface-templated asymmetric modification. Sequential vacuum filtration[28] and electrospinning[29] are the most widely applied strategies for bi-layer compositing. In some cases, Janus membranes are fabricated by directly filtrating nanomaterials[30] or electrospinning nanofibers[31,32] onto an existing substrate with opposing properties. Other conventional membrane-forming methods, such as phase inversion, can also be utilized to fabricate bi-layer membrane structures in principle. Whether a method is suitable for direct compositing depends on the characteristic pore size and layer thickness associated with that method. Single-sided spray coating can be regarded as either a bi-layer compositing strategy or an asymmetric modification approach, depending on whether the pores are generated from the spraying layer or merely narrowed by this coating. Additive manufacturing techniques, such as 3D printing, offer significant potential for fabricating bilayer structures with precise control over pore architecture.[33] These approaches not only enable fine-tuning of membrane properties but also provide an ideal platform for investigating mass transport behavior within Janus membranes.[34] However, the current resolution of 3D printing technologies results in pore sizes that are still too large, limiting the applicability of this technique for membrane construction at present.

Asymmetric modification offers an alternative strategy for fabricating Janus membranes, enabling the creation of both bilayer and gradient structures. Considering that most modification methods are carried out in solution, the primary challenge lies in preventing modification throughout the entire membrane due to capillary penetration and spreading within the porous structure. An interface-assisted strategy has been developed to fabricate bilayer Janus membranes, with the liquid-gas interface being the most commonly utilized.[11] Typically, a hydrophobic membrane is floated on the modification solution, allowing modification to occur only on the side in contact with the solution. Mussel-inspired chemistry based on polydopamine or polyphenols is widely employed due to its advantages in hydrophilizing hydrophobic surfaces.[35] Hydrophilic membranes are rarely used as substrates in this method due to their susceptibility to wetting by solutions. While some researchers have attributed liquid-gas interface-assisted modification to a buoyancy-assisted mechanism,[36,37] it is surface tension-rather than buoyancy-that stabilizes the membrane at the gas-liquid interface in most cases. Solid-liquid[38] and liquid-liquid[39] interfaces have also been explored for fabricating such membranes.

In contrast, gradient Janus membranes are generally achieved through diffusion-controlled asymmetric modification. In this process, an energy or mass gradient is applied across the membrane. For example, light intensity decreases with depth into the membrane, so light-triggered reactions, including photo-crosslinking[13] and photo-degradation,[40] can be used to induce asymmetric modification. Additionally, reactive vapor diffusion through the membrane pores provides another means to achieve gradient modification.[41] Hydrophilic membranes are typically used as substrates in this strategy due to the relatively high reactivity of their surface. Chlorosilanes with long alkyl or fluorinated chains serve as the reactive vapor to react with polar groups.[42] Single-sided atomic layer deposition (ALD) has also been applied to fabricate gradient Janus membranes as a precise vapor deposition technique.[43] Diffusion-controlled asymmetric modification can also be performed in the liquid phase, such as through asymmetric deposition under an electric field.[44] As mentioned above, single-sided spray coating can be also regarded as a gradient modification strategy when modifying macro-porous substrates, such as fabrics or meshes, in which the gradient structure forms due to the gradual penetration of the reactive solution.[45]

Janus membranes with opposing surface charges are also constructed using the principles mentioned above. Bi-layer composite strategies are commonly employed in fabricating these membranes, as the opposing surface charges are typically achieved by using different materials. It is worth noting that these membranes are typically characterized by nanopores, and their layers are usually fabricated through methods such as microphase separation of block copolymers, self-assembly of nanomaterials, or interfacial polymerization.[46] Asymmetric modification might also be applied to create such membranes. It is worth noting that these membranes are generally hydrophilic to facilitate liquid infiltration, preventing the spontaneous formation of a gas-liquid interface. Diffusion-controlled modifications are more suitable for fabricating this type of Janus membrane.

2.2. Structure Regulation

Adjusting the thickness of each layer is crucial for Janus membranes, as both the individual thickness and the thickness ratio of layers influence the transport behavior and resistance. For example, a critical thickness of the hydrophobic layer is necessary to enable unidirectional liquid transport.[47]

Bi-layer compositing strategy appears to be the most promising approach for adjusting the thickness of each layer. For example, sequential electrospinning of nanofiber membranes has been widely employed in laboratories to fabricate Janus membranes with adjustable thickness ratios.[48] Hydrophilic polymers, such as polyvinylidene fluoride (PVDF), are used to form the hydrophobic layer, while hydrophilic polymers like polyacrylonitrile (PAN) are used to construct the hydrophilic layer.[49] The nanofiber thickness can be controlled by adjusting parameters such as polymer concentration, applied voltage, electrospinning duration, etc. It is important to note that the pores within these membranes, which result from fiber stacking, become non-uniform when the layer is excessively thin. The transport behavior of liquid through a Janus membrane is closely linked to both pore size and layer thickness. In such cases, the controllability of the method may be compromised. Furthermore, the compatibility between the two layers presents a significant challenge, which will be discussed in the following section. Other bi-layer compositing methods can also adjust layer thickness, as the two layers are fabricated independently. As mentioned above, Janus membranes with opposing surface charges are primarily fabricated through bi-layer compositing methods. Unlike most hydrophilic-hydrophobic Janus membranes with micron-sized pores, these membranes typically feature nanopores. The self-assembly of block copolymers can be used to create uniform, straight nanopores, with pore size adjustable by the structure of the block copolymers. The surface charges of the pores are determined by the chemistry of the blocks that form the pores. Stacking 2D nanosheets is another widely used approach for constructing such membranes, where the channel width between layers can be controlled using molecular or nanoparticle “spacers”.[50] Beyond pore size and geometry, surface potential is another crucial parameter that influences transport phenomena within membranes, which can be modulated by adjusting the type and density of functional groups.

Interface-assisted asymmetric modification presents inherent challenges in precisely controlling the thickness of individual layers. However, in practice, the thickness of the modifying layer can be tailored by adjusting the modification conditions. For instance, in mussel-inspired single-sided deposition, extending the deposition time leads to a thicker hydrophilic layer as the wetting front moves with the deposition process, which can be attributed to the increased hydrophilicity over time.[35] In addition, Lee *et al.* demonstrated a method to adjust layer thickness by filling the pores of an anodic aluminium oxide (AAO) membrane with a photoresist.[51] By varying the etching time, they controlled the position of the solid-air interface, thereby adjusting the thickness available for modification. The solid-liquid or solid-gas interface is generally easier to regulate than the gas-liquid or liquid-liquid interface.

For gradient Janus membranes, while there is no distinct boundary between the hydrophilic and hydrophobic layers, a liquid-gas interface naturally forms upon contact with water. Diffusion-controlled modification offers a means to tune the wettability gradient by regulating diffusion time, with the gradient resulting from the interplay between surface reaction kinetics and diffusion dynamics. In conventional approaches, Janus membranes are typically fabricated by exposing the material to reactant vapor, which makes precise control over modification depth challenging. ALD, however, enables precise, atomic-scale conformal modification, offering superior control over gradient construction.[52] The diffusion behavior of precursor vapors during ALD is influenced by the pore size and tortuosity of membranes. When the mean free path of the precursor vapors significantly exceeds the pore size, their transport is governed by Knudsen diffusion. The modification profile is ultimately determined by the competition between deposition reactions and diffusion processes, which can be quantified using the Damköhler number $\alpha = 3/2(AR)^2\beta_0$ in a model straight pore.[53] AR represents the aspect ratio and β_0 demotes the initial sticking probability. When $\alpha \geq 100$, a gradient coating is more likely to form. Thus, various parameters in ALD, such as precursor reactivity, temperature, dose time, and deposition cycles, can be tuned to adjust the modification gradient. Damköhler number can also serve as a guide for selecting other diffusion-controlled modification systems.

2.3. Scalability Potential

Despite the development of numerous methods for fabricating Janus membranes in recent years, scaling up their production remains a challenge, creating a gap between scientific research and practical applications. Bi-layer compositing strategies offer a more straightforward pathway for translating laboratory-scale methods into industrial membrane production technologies through a sequential fabrication process (Figure 2b). For instance, as previously mentioned, sequential electrospinning is the most commonly employed method for laboratory-scale fabrication of Janus membranes.

With advancements in industrial electrospinning technologies, such as needleless spinning and roll-to-roll processing, large-scale production of Janus nanofiber membranes has become feasible. Additionally, constructing membrane layers on a porous substrate with opposing properties presents another industrially viable approach for large-scale production. A key challenge in this approach lies in the poor compatibility between the two layers with opposing properties, which often leads to delamination during application. The two layers can be effectively bonded through methods such as hot pressing or spot welding industrially. Specifically, additive manufacturing enables precise design and regulation of microstructure and properties, which could become a promising approach for scaling up Janus membranes, provided that the issue of fabrication accuracy can be resolved.

Single-sided spraying coating is another method with the potential for scale-up. However, it is more suitable for the fabrication of Janus fabrics or meshes with larger pores, rather than Janus microfiltration or ultrafiltration

membranes, as the sprayed coatings tend to cover smaller pores more easily. Other single-sided modification strategies, such as plasma treatment or surface grafting, may also hold potential for scale-up.

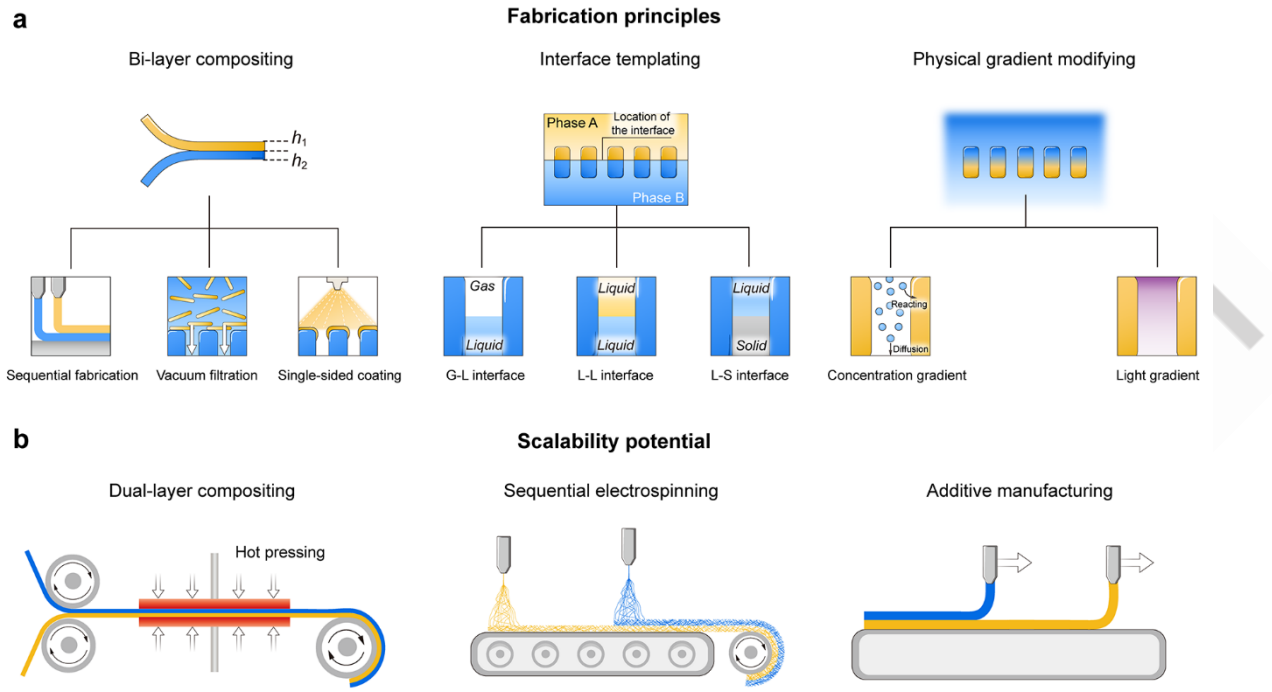

Figure 2. Construction of Janus membranes. **a.** Fabrication principles and structure regulation of Janus membranes. **b.** Potential scaling-up strategies for Janus membranes.

3. Physics behind Janus Superiority

The superiority of Janus membranes or devices originates from distinct physics behind at different scales. For Janus membranes with pore sizes ranging from sub-micron to tens of microns, their advantages typically arise from five key elements: two surfaces with opposing properties, two porous layers with contrasting characteristics, and the interface between these layers. Surfaces with opposing wettability create distinct liquid or gas contact angles, resulting in a Laplace pressure difference across the membrane that drives directional liquid movement. Laplace pressure on each surface can be described by the equation

$$\Delta P = 2\gamma \sin\theta_d / r_d$$

where γ represents the interfacial tension, θ_d and r_d are the contact angle and radius of the droplet. It is worth noting that the maximum Laplace pressure on the membrane surface is reached at a contact angle of 90°.

Unidirectional liquid transport is a characteristic phenomenon primarily governed by this force, which includes three stages: liquid intrusion, capillary wetting, and liquid transport (Figure 3a).[47] Taking water transport through a hydrophilic-hydrophobic membrane as an example, the initial intrusion of liquid from the hydrophobic layer into the hydrophilic layer is a critical step. Typically, the hydrophobic layer needs to be sufficiently thin to allow the directional transfer of water droplets. Some studies propose that when the hydrophobic layer is thin enough, the attraction of the hydrophilic layer to the liquid causes its breakdown. However, many studies show that, during directional transfer, the thickness of the hydrophobic layer ranges from several microns to tens of microns, which presents a significant scale gap in intermolecular interactions. Other studies attribute the formation of water channels to capillary condensation within the hydrophilic channels, yet many of these studies involve Janus membranes or fabrics with relatively large pore sizes, where capillary condensation effects are minimal. Additionally, some researchers believe that the directional transfer phenomenon in Janus membrane materials results from inhomogeneities in their preparation process. Specifically, hydrophilic channels may exist within the hydrophobic layer, providing pathways for water droplet transfer.[54] Recent work demonstrates that, for a bi-layer configuration, the liquid intrusion is driven by a direct-contact mechanism, while in a gradient configuration, the movement of the triple-phase contact line along the surface tension gradient serves as the driving force.

Once the water reaches the hydrophilic layer, its transport is governed by capillary forces within the pores, which can be described by the following equation

$$\Delta P = 2\gamma \cos\theta_p / r_p$$

where θ_p is the contact angle on the pore wall and r_p is the pore radius. The capillary force is significantly larger than the Laplace pressure exerted by droplets on the membrane surface, thereby dominating the capillary wetting stage. The maximum capillary force occurs when the contact angle is 0° within hydrophilic channels.

Once the lyophilic layer is saturated with water, the Laplace pressure of the droplets becomes the dominant driving force. In most cases, liquid transport within the Janus membrane is governed by bulk flow, which follows Darcy's law, or more precisely, the Hagen–Poiseuille law. The flow velocity v within a straight, cylindrical pore can be described by the Hagen-Poiseuille equation[55]

$$v = (D^2/32\mu L)\Delta P$$

where D is the pore diameter, μ is the fluid viscosity, L is the membrane thickness and ΔP is the pressure difference. For membranes with tortuous pores, L is given by $\tau \cdot l_m$, in which τ is tortuosity and l_m is membrane thickness. Janus membranes with larger pore sizes and lower tortuosity exhibit higher flow rates during liquid transport accordingly. To accelerate liquid transport through Janus membranes, one approach is to design membranes with large, straight, and hydrophilic pores. Alternatively, coupling a liquid removal process, such as evaporation, at the permeate side can maintain transport in the capillary wetting stage.

The porous layers exhibit varying resistance to liquid transport. Even for pores with identical structures, surfaces with different properties result in distinct interactions between water molecules and pore walls. Notably, the intrusion pressure required for liquid entry into each layer plays a crucial role in liquid transport, as reflected by the Laplace equation within the pores. In addition, the hydrophilic-hydrophobic interface defines the locations of both the gas-liquid and liquid-liquid interfaces.

At a static interface, the diffusion of molecules or ions in liquid or gas phase follows Fick's law, while the distribution between the two phases typically adheres to Henry's law, Raoult's law or Nernst distribution law (Figure 3b). In the lyophilic layer, diffusivity through pores in a liquid phase can be modified by a restrictive factor[56]

$$K_r = (1 - d_m/d_p)^4$$

in which d_m and d_p are molecule and pore size respectively. In the lyophobic layer, gas or vapor molecules diffuse through pores via Knudsen diffusion, molecular diffusion, or a combination of both, which is determined by Knudsen number[57]

$$K_n = \lambda/d_p$$

where λ is the mean free path of the molecules. In particular, the evaporation process can be modeled by Hertz–Knudsen relation with correction terms and empirical constants.[58]

For Janus membranes with nano or sub-nano pores, the Janus superiority originated from the nano-sized effects on molecule or ion transport within the pores (Figure 3c). The curved liquid-vapor interface causes significant changes in vapor pressure within nanopores, as described by the Kelvin equation[59]

$$\ln(p_r/p_{sat}) = 2\gamma V_m/rRT$$

where p_r and p_{sat} are the actual vapor pressure of a curved surface and saturated vapor pressure of a flat surface respectively, V_m is the molar volume of the liquid, and r is the radius of the droplet. In hydrophilic nanopores, the curvature is concave, and p_r is lower than p_{sat}, which facilitates capillary condensation; conversely, in hydrophobic nanopores, the curvature is convex, and p_r is higher than p_{sat}, promoting capillary evaporation. This phenomenon can be further extended to atomic-scale channels.[60]

Furthermore, the surfaces of the pore walls contribute significantly to the overall pore volume, and their interactions with molecules or ions—such as hydrogen bonding with water molecules or electrostatic interactions within the Debye length—are crucial to consider. The former is believed to influence the evaporation enthalpy of water molecules, while the latter affects ion distribution within the channel, which can be modeled using the Poisson-Nernst-Planck equation.[61] Considering the distinct physical principles underlying different separation systems, further details will be discussed in the following sections

When Janus properties are extended to a spatial structure or membrane system, Janus superiority typically arises from the interplay between different processes facilitated by materials with distinct properties. Conventional membrane separation suffers from concentration polarization, a challenge that can potentially be mitigated by introducing a pair of separation processes that can continuously remove different components. Therefore, the superiority of Janus macro-systems lies in their integration of several fundamental physical principles at the macroscopic scale, rather than merely basic physics at the microscopic scale. In this Review, we discuss how a two-dimensional channel composed of hydrophilic and hydrophobic membranes achieves a positive, synergetic effect in separation.

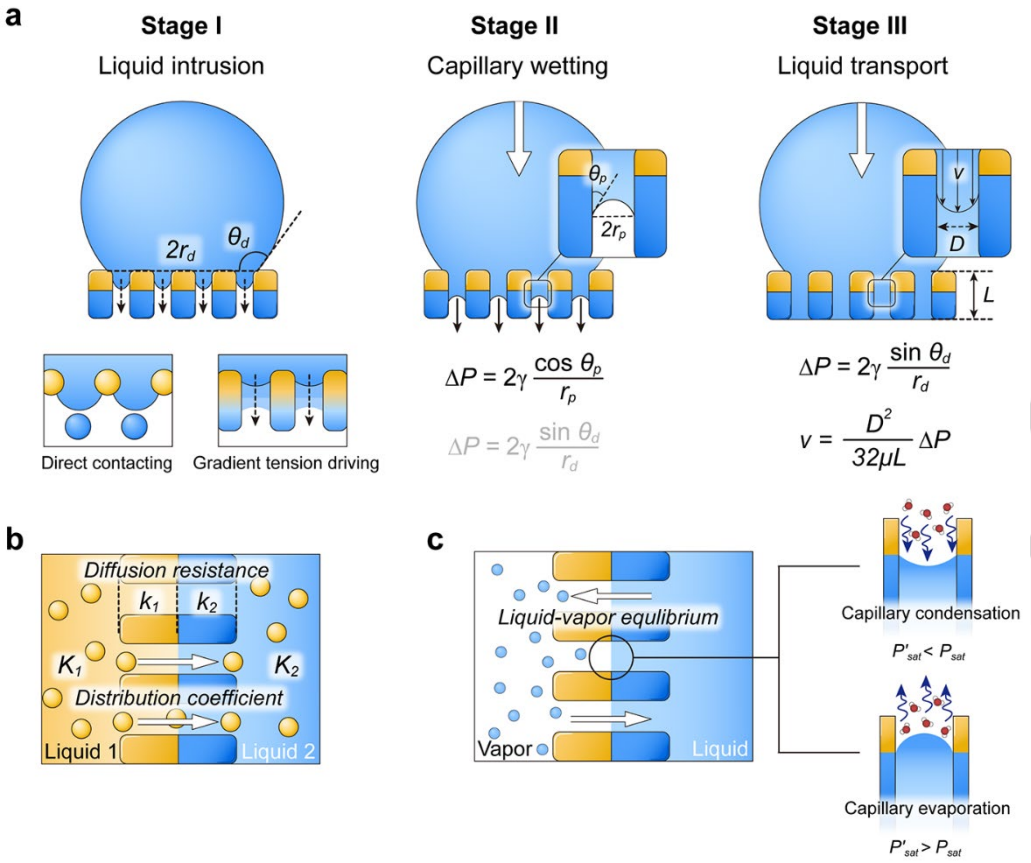

Figure 3. Physics behind Janus superiority. **a.** Unidirectional transport mechanisms of fluids on Janus membranes. **b.** Transport parameters between two phases with a Janus membrane. **c.** Capillary evaporation and condensation within a Janus nanochannel.

4. Janus Superiority in Phase Transfer

The unique properties of Janus membranes make them well-suited for phase-to-phase transfer processes, representing some of the earliest examples of Janus superiority. These processes can take advantage of the distinct properties on each side of the membrane to meet the contrasting requirements of different phases within the same application. Compared to traditional homogeneous membranes, Janus membranes normally exhibit superior properties in these two-phase applications. Based on the nature of these processes, the application scenarios can be categorized into coalescence and dispersion.

4.1. Coalescence: Merging Interfaces

Coalescence involves the transition from a dispersed phase to a continuous phase (Figure 4a). Applications such as demulsification, defoaming, and fog collection fall under this category. This process is typically spontaneous from a thermodynamic perspective, as surface energy is released when interfaces merge into a larger dispersed or even a continuous phase. The difference in wettability between the two sides of the Janus membrane leads to a disparity in interface curvature, resulting in a Laplace pressure difference. This pressure difference promotes the one-way mass transfer of the target liquid (or gas) from the lyophobic (or aerophobic) side to the lyophilic (or aerophilic) side, and this driving force can be described as

$$\Delta P = 2\gamma\left(\frac{\sin\theta_{phobic}}{r_{phobic}} - \frac{\sin\theta_{philic}}{r_{philic}}\right)$$

where γ represents the interface tension, θ_{phobic}, θ_{philic} are the contact angles on lyophobic (aerophobic) and lyophilic (aerophilic) surfaces, and r_{phobic}, r_{philic} are their diameters of curvature. When the permeate side is in a bulk phase, the Laplace pressure on that side disappears. For example, in fog collection, water droplets are collected on the hydrophobic side, merged, and then transported to the hydrophilic side.[14] In demulsification processes, the hydrophilic/oleophobic surface of the Janus membrane faces towards the dispersed oil phase, and the emulsions

coalesce and migrate to the hydrophobic/lipophilic side.[13] It is important to note that in emulsions, the dispersed phase is typically stabilized by surfactants. Therefore, a hydrophilic surface with charges opposite to those of the surfactant is generally required to effectively demulsify the emulsions.[62] This process can also be applied to remove dispersed gas from a bulk liquid. For instance, Janus channels can effectively remove hydrogen bubbles generated by an electrode during the water electrolysis reaction.[63]

It is worth noting that the coalescence process relies on the unidirectional liquid transport capability of the Janus membrane. Therefore, this process could be also utilized to separate a small amount of liquids like blood plasma,[64] or pump sweat for wet-thermal management[65] and biofluid for wound healing.[66] The driving force from the Laplace pressure difference is effective only in the presence of a curved liquid-liquid or liquid-gas interface. Once separation occurs within a continuous phase, the facilitated transport through the membrane becomes ineffective. Another important point is that when the membrane is in a dried state, the capillary forces within the pores are significantly stronger than the Laplace pressure of the droplets, which governs liquid transport as a wetting process. In contrast, when the membrane is saturated with liquid, the Laplace pressure takes precedence in driving the transport.[47] Recently, thermo-responsive polymers have been integrated into Janus wound dressings or fabrics to enable smart management of exudate and sweat drainage in response to specific moisture or temperature conditions.[67,68]

From an energy conversion perspective, Janus membrane converts surface energy into kinetic energy during coalescence. By harnessing this energy, researchers have developed water engines capable of directly propelling micro-boats.[69] Notably, the direction of motion is opposite to that of liquid transport. Moreover, this energy can also be transformed into electrical energy. When a saline solution (e.g., sweat or seawater) flows through conductive membrane channels, it generates a flow potential via classical electrokinetic reactions.[70] The total energy generated from this process must not exceed the surface energy of all the dispersed droplets, represented as $E_{surf} = \sum_{n=1}^{N} 4\pi\gamma\, {r_n}^2$, where r_n is the radius of each droplet. Membrane resistance leads to energy loss during the conversion of surface energy into kinetic energy, so the maximum energy output should be repsented as $E_{out} = \eta \sum_{n=1}^{N} 4\pi\gamma\, {r_n}^2$. The conversion efficiency η could be estimated by measuring the kinetic energy of the liquid flowing through the pores or the output of electric energy. However, a quantatitive description of the energy conversion is still lacking.

4.2. Dispersion: Creating Interfaces

Dispersion is the inverse process of coalescence, which involves the transition from a continuous phase to a dispersed phase (Figure 4b). Applications such as emulsification, aeration, and spraying fall under this category. Unlike coalescence, dispersion requires energy input to create new interfaces. In this process, the liquid (or gas) is transferred from the lyophilic (or aerophilic) side to the lyophobic (or aerophobic) side. The entering interface is normally lyophilic or aerophilic to facilitate the entry of liquid or gas, while the departing interface is lyophobic or aerophobic to cause a large contact angle and quick detachment from the surface. Energy consumption arises from both generating new interfaces and overcoming membrane resistance. While the former is essential, the latter can be reduced. The transport resistance within the membrane can be described as follows:

$$\Delta P_{loss} = LC_1 J^{C_2}$$

where *L* represents the thickness of the layer, J is the mass flux, C_1 is the pore structure coefficient, which is determined by factors such as pore size distribution, porosity, and other relevant parameters, while C_2 is a liquid property coefficient, which depends on factors like flow rate, viscosity, and other related properties. The lyophilic or aerophilic of Janus membrane plays a crucial role in reducing transmission resistance within the membrane, thereby minimizing overall energy consumption. For example, in membrane aeration, the hydrophilic surface of the Janus membrane faces the liquid phase, facilitating quick gas release and the formation of smaller bubbles.[11,71] The hydrophobic surface faces the gas phase, preventing liquid penetration and reducing air resistance during gas passage, thus reducing energy consumption. The operating pressure of a Janus membrane is significantly lower than that of a uniform hydrophilic membrane. Janus membranes used for emulsification share the same principles and advantages as those used for aeration. By switching the direction of dispersion, either oil-in-water or water-in-oil emulsions can be prepared through a Janus membrane.[12] In principle, the minimum energy consumption is achieved when the entering layer occupies the entire thickness of the membrane, while the departing layer is confined to the membrane surface. Moreover, by coupling emulsification with a subsequent polymerization reaction, Janus membrane can produce dispersed microspheres through dispersion.[72]

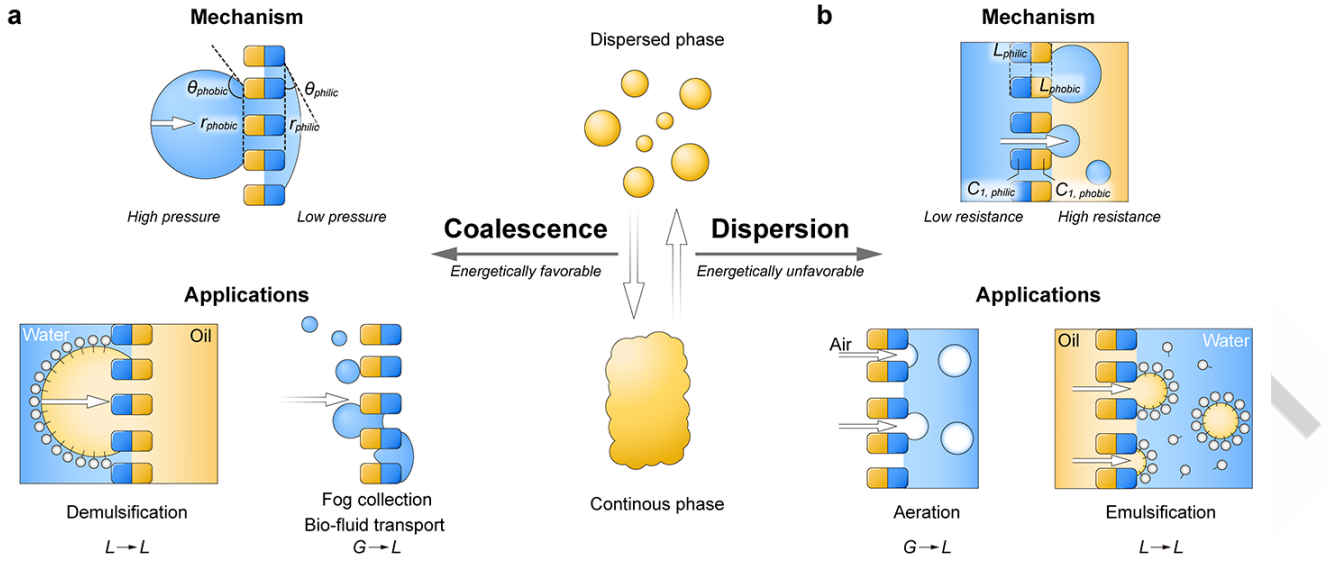

Figure 4. Janus superiority in phase transfer. **a.** Coalescence processes facilitated by Janus membranes. **b.** Dispersion processes enhanced by Janus membranes.

5. Janus Superiority in Ionic/Molecular Transport

Regarding the Janus superiority in ionic or molecular transport, it can be categorized into two situations: 1) transport occurring between two phases, where the Janus membrane typically features much larger pores than the ions or molecules; and 2) transport occurring in a homogeneous phase, where the pores within Janus membranes are comparable in scale to the ions or molecules. In the first case, Janus membrane normally acts as a role of interface regulation. It is worth mentioning that the membranes used in these processes have pore sizes ranging from micrometers to sub-nanometers. For membranes with micron pores, the role of Janus membrane is to create an interface facilitating interphase molecular transport. When the pores are in the nano or sub-nanometer range, bulk flow converts to nanoconfined fluid, where interactions between the channel surfaces and molecules/ions govern the transport behavior within the membranes.[73] The mass and energy transport characteristics are strongly influenced by nanoscale effects, including surface effects, size-dependent phenomena, quantum effects, and others.

5.1. Interphase Molecular Transport

This process involves molecular transfer between two phases without phase transfer (Figure 5a). Applications such as membrane distillation,[16,74] membrane contactor[75,76] and membrane extraction[77,78] fall under this category. The Janus membrane regulates the position of the interface, thereby reducing mass transfer distance or stabilizing the interface. For instance, in membrane extraction, a liquid-liquid mass transfer process, the Janus membrane transfers the liquid-liquid interface from the outside to the inside of the membrane, enhancing interface stability during cross-flow operation.[77] In membrane distillation, the gas-liquid interface migrates from the outside to the inside of the membrane. This migration ensures reduced steam mass transfer resistance while maintaining heat transfer resistance.[16] It is important to note that many studies have also utilized Janus membranes to mitigate oil fouling during membrane distillation.[74,79] In these cases, the hydrophilic/oleophobic side typically faces the feed to prevent oil adhesion. Additionally, some research fabricated a dense hydrophilic film on a hydrophobic substrate to reject surfactants and avoid unfavorable wetting of it.[80] It is worth noting that these designs do not leverage Janus structure to enhance mass transfer.

Recently, many research groups have applied Janus structures in interfacial solar-driven evaporation, a process similar to membrane distillation that also involves liquid-to-gas (vapor) mass transfer.[81] In a conventional configuration, the hydrophilic side faces the feed, while the hydrophobic side is oriented toward the light source. The evaporation interface is situated within the membrane. The hydrophilic layer pumps water to the evaporation interface, while the hydrophobic photothermal layer prevents scaling on the membrane surface that may obstruct light absorption and energy conversion.[17] Although the scaling issue on the top surface is resolved, scaling within the membrane remains a challenge. A Janus membrane with a moving interface can address this problem, in which the photothermal hydrophobic layer is constructed using a thermo-responsive polymer, poly(N-isopropyl acrylamide) (PNIPAM).[82] The membrane exhibits Janus properties during the daytime but becomes fully

hydrophilic at night. In recent research, the Janus membrane has been flipped over, in which the bottom hydrophobic layer filled with air can serve as a thermo-insulating layer to promote heat management.[29] In certain suspended configurations, the Janus structure has also been utilized to mitigate scaling by regulating the deposition position[83] or facilitating de-scaling through a seesaw mechanism.[84] Recent research has explored the use of photothermal Janus membranes in membrane distillation to mitigate temperature polarization at the evaporation interface to enhance the driving force of this process.[85]

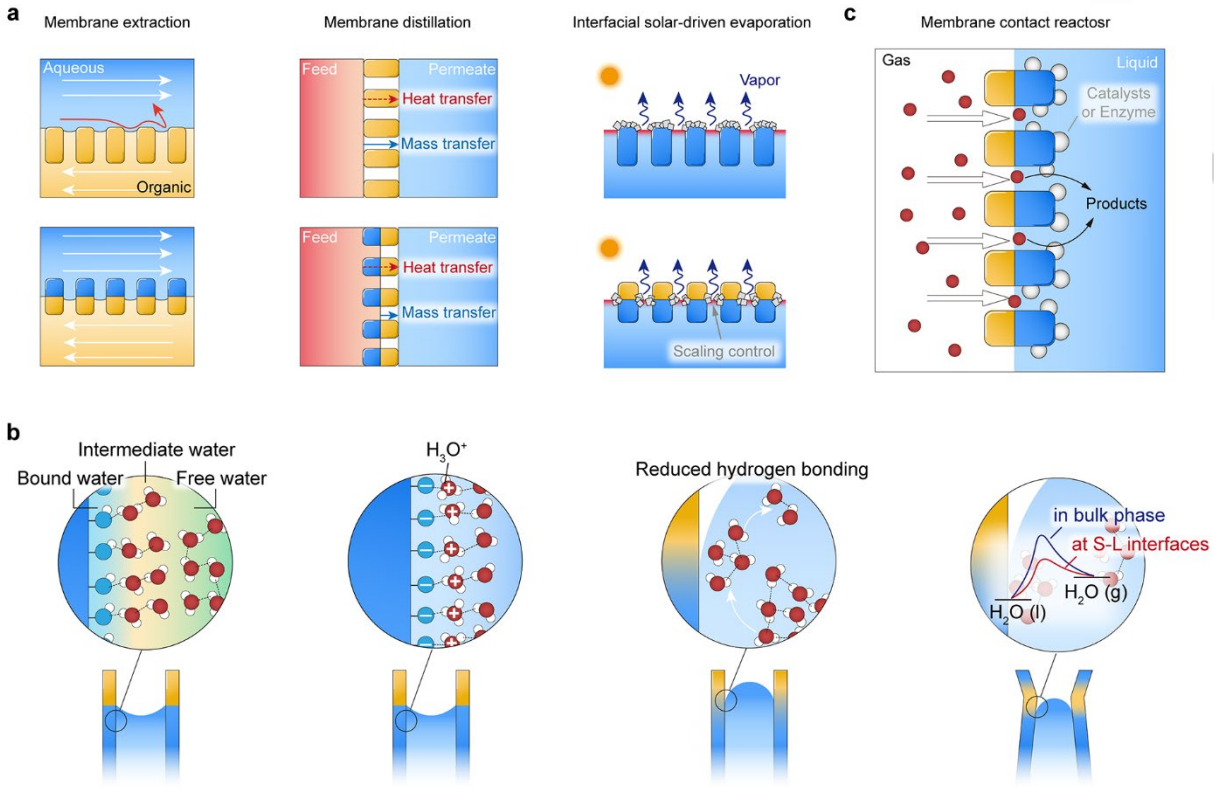

Figure 5. Janus superiority in interphase molecular transport. **a.** Comparison of Janus membrane with uniform membranes in membrane extraction, distillation, and solar evaporation. **b.** Proposed mechanisms of evaporation enhancement within Janus nanochannels. **c.** Janus superiority in a transport-reaction coupled process in membrane contact reactors.

In addition to interface regulation, recent advancements have revealed the significant size effects on evaporation dynamics within Janus membranes (Figure 5b). Some researchers attributed the enhanced evaporation to the interactions within hydrophilic pores. For example, Janus membranes, constructed with AAO and featuring straight-through pores, exhibited a notable increase in evaporation flux from 1.95 to 2.18 $kg \cdot m^{-2} \cdot h^{-1}$ as the pore size was reduced from 200 nm to 20 nm.[86] This phenomenon is attributed to the abundance of hydroxyl groups on the hydrophilic pore walls, which weaken hydrogen bonding among water molecules and create an intermediate layer between bound and free water. As the pore size decreases, the proportion of this intermediate water increases, leading to a decrease in the enthalpy of evaporation. Additionally, some studies attribute the enhanced evaporation kinetics to surface-charge-induced changes in the concentration of hydronium ions within the nanopores.[87]

Conversely, researchers also found the number of hydrogen bonds diminishes within nanoconfined hydrophobic channels of several nanometers, further lowering the evaporation enthalpy due to the reduced interaction energy of water.[88] The utilization of vertically aligned carbon nanotubes in these channels illustrates how nanoscale hydrophobic environments can facilitate rapid evaporation. It is important to note that lowering the enthalpy of vaporization does not necessarily lead to improved efficiency during continuous evaporation, as the thermodynamic states before entering and after exiting the evaporator remain unchanged. Moreover, the hypothesis of reduced vaporization enthalpy has been met with considerable skepticism.[89] Recent studies suggest that, in such cases, water may evaporate as clusters rather than as individual molecules.[90] In fact, prior to these findings, Wang's group has innovated a covalent organic framework (COF) membrane characterized by vertically aligned channels (~2 nm) with gradient hydrophilicity.[91] Molecular dynamics simulations indicate that evaporation at solid-liquid interfaces encounters a significantly lower energy barrier of evaporation compared to that in the bulk phase, and the presence of straight pores also contributes to the rapid water transport to the evaporation interface. Such a COF membrane exhibits exceptionally high flux in membrane distillation, achieving around 200 $L \cdot m^{-2} \cdot h^{-1}$ at a relatively low feed temperature of 65 °C. Since most Janus membranes have pore sizes ranging from several

hundred nanometers to several microns, these findings provide new insights into the specific mass transfer behavior at the nanoscale within a Janus membrane, representing a promising direction in this field.

Beyond liquid-to-gas (vapor) molecular transport, the inverse process—gas-to-liquid molecular transport—has also garnered significant attention in recent research. Such a membrane apparatus is normally called a membrane contactor (Figure 5c). Conventional membrane contactors are typically fully hydrophobic to create a liquid-gas interface. The hydrophilic-hydrophobic interface plays a similar role in re-locating the gas-liquid interface, akin to its function in membrane distillation. According to the two-film theory, the concentration of dissolved gas molecules is relatively high near the interface. By coupling with subsequent reactions, Janus membrane contactor can serve as a reactor to convert these molecules into other products. In these cases, catalysts are typically immobilized in the hydrophilic layer to facilitate reactions at the triple-phase line.[15,92,93] This system overcomes the limited solubility and mass transfer of O_2 in an aqueous phase, facilitating the mineralization of organic contaminants[94] and the reduction of O_2 to H_2O_2.[15] Similarly, biocatalysts such as enzymes, which require an aqueous environment, were immobilized on the hydrophilic layer of a Janus membrane, functioning as a reactive membrane contactor.[75,76] Moreover, the excellent biocompatibility of the hydrophilic layer in the Janus structure is crucial for membrane contactors used in medical applications, such as extracorporeal membrane oxygenation.[95]

5.2. Homogenous Molecular/Ionic Transport

Janus membranes with opposing wettability typically create an interface between two phases due to their intrinsic surface energies. As a result, most of these membranes govern interphase transfer or molecular transport across phases, as mentioned above. Polyester membranes with integrated Janus pathways have recently been synthesized via interfacial polymerization between cyclodextrin (CD) and trimesoyl chloride.[96] Cyclodextrins feature intrinsic non-polar cavities and polar channels in outer space, enabling the selective transport of non-polar and polar liquids through distinct pathways. This work highlights the advantages of a hybrid hydrophilic-hydrophobic structure in molecular transport, which contrasts with the previously discussed Janus structures that switch wettability along the transport path. Notably, recent findings suggest that both polar and non-polar liquids are unable to pass through the cavities of CDs.[97] Further investigation is needed to elucidate how this hydrophilic-hydrophobic microstructure contributes to molecular transport dynamics. Regarding ion transport, some studies also highlight the potential to regulate reactive crystallization by controllable ion transport within Janus membranes with opposing wettability.[98] However, it appears that the Janus membrane primarily functions to modulate the reaction interface, rather than directly controlling ion transport.

Nanochannels with asymmetric geometries or surface charge distributions exhibit a significant asymmetric ion transport behavior.[99] As the channel size approaches the Debye length, the passage of counterions is favored over co-ions due to electrostatic interactions between the ions and the charged channel walls. When an electric field is applied, these nanochannels allow preferential ion flow in one direction while effectively suppressing flow in the opposite direction, a phenomenon known as ionic rectification (Figure 6a). This behavior is also observed in nanopore Janus membranes with opposing surface charges, and can be quantitatively described by the Poisson–Nernst–Planck equation. The rectifying effect arises from the accumulation or depletion of ions within the channel, depending on the applied bias polarity, which corresponds to the 'on' and 'off' states of a diode.[100] Recent studies have shown that ion rectification is not limited to channels with radii smaller than the Debye length.[61] The ion rectification provides the foundation for osmotic energy harvesting. The osmotic energy generated from the mixing of river and seawater at the outfall can be harvested through reverse electrodialysis.[101] Homogeneous ion-exchange membranes typically suffer from poor mass transport due to their sub-nanometer pores and the energy loss associated with ionic concentration polarization. In contrast, Janus membranes offer a significant advantage with their relatively large pores and ion rectification capabilities, which help prevent ion accumulation at the dilute end of the membrane.[102] Asymmetric pore sizes are also commonly used to further enhance membrane performance. Concerning membrane thickness, a thinner membrane reduces resistance to ion transport but may compromise ion selectivity. Therefore, an optimal thickness must be selected to balance these competing factors. Additionally, it is important to note that the Debye length decreases sharply as electrolyte concentration increases, which should be considered when designing membranes.[103]

A recent study reported the development of a Janus microporous membrane consisting of donor and acceptor layers, which efficiently facilitates charge separation upon light exposure (Figure 6b).[104] This process generates a transmembrane potential that drives active and selective ion transport through the membrane. Such Janus membranes offer a novel approach to enable directional ion transport in response to external energy inputs.

Beyond selective ion transport, Janus nanofiltration membranes with a composite selective film, incorporating both positively and negatively charged layers, have been developed to reject both divalent cations and anions based on the Donnan effect (Figure 6c).[105] For the separation of mono-/divalent ions, the top layer with same charges can reject the divalent ions while the bottom layer with opposing charges facilitate the transport of monovalent ions. Moreover, monovalent counterions may accumulate at the interface that enhances the “shielding effects”.[106] Despite their promising potential in nanofiltration applications, key questions remain, such as the effective distance over which a charged surface can influence ion rejection.

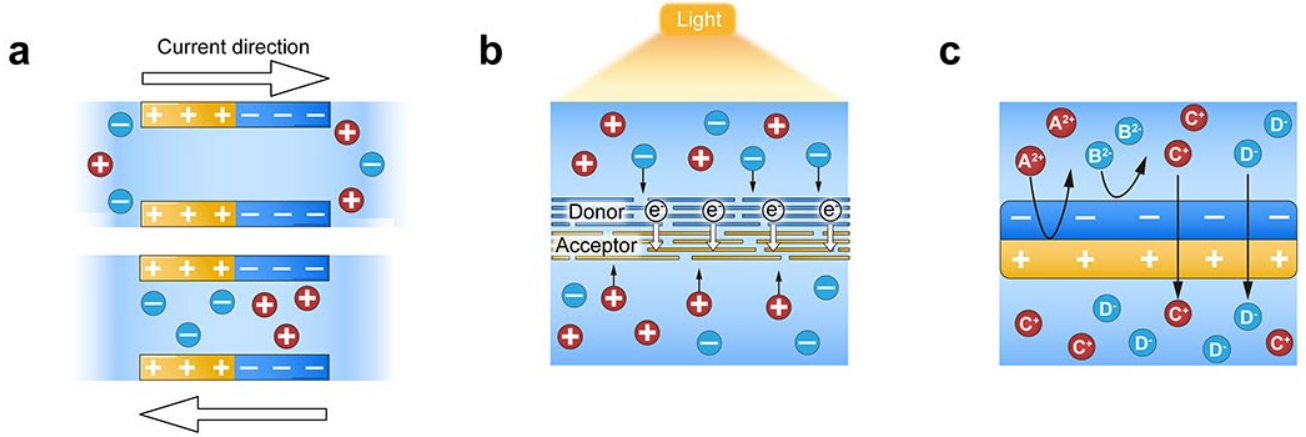

Figure 6. Janus superiority in Homogenous molecular/ionic transport. **a.** Ionic rectification within Janus membranes with opposing surface charges. **b.** Light-triggered directional ion transport within a Janus membrane. **c.** Janus membranes with opposing surface charges for nanofiltration.

6. Janus Superiority in Macro-Separation Systems

The concept of Janus superiority has been demonstrated on a significantly larger scale, particularly in spatial structures exhibiting Janus properties. A Janus channel, consisting of a hydrophilic membrane paired with a hydrophobic membrane, has been developed to enable the concurrent recovery of water and oil from emulsions (Figure 7).[107] The narrow channel between the membranes is crucial for enhancing separation efficiency; within this confined space, emulsions become substantially enriched as water permeates through the hydrophilic membrane. Concurrently, collisions among oil droplets are intensified, promoting coalescence and subsequent demulsification through the hydrophobic membrane. Remarkably, the interplay between the two membranes exemplifies Janus superiority at the separation system scale. In conventional separation systems utilizing a hydrophilic membrane, water permeates while oil is rejected at the feed side, resulting in a monotonous increase in oil concentration. This process often leads to concentration polarization, causing a decline in water permeation flux over time. Similarly, membrane demulsification systems employing a hydrophobic membrane monotonically decrease the oil content in the feed, ultimately experiencing an oil flux decline as separation progresses. In contrast, the Janus channel can remove both water and oil simultaneously from the system. Consequently, the accumulation of oil droplets facilitates oil removal, while the removal of oil facilitates water permeation. Such a feedback loop can promote both water and oil recovery compared to a single-membrane system. This research demonstrates the potential of extending Janus superiority on a macro-separation system. Notably, electrodialysis or reverse electrodialysis serves as a well-established example of a “Janus system” consisting of a pair of positively charged and negatively charged membranes, although its operating principles differ significantly from those of the Janus channel described here[108,109]

Beyond the spatial Janus structure, Janus properties in a temporal sequence demonstrate superiority in separating multiphase systems, such as oil/water emulsions. A single hydrophilic membrane module facilitates water permeation while concentrating emulsions, resulting in a significant reduction in flux. In contrast, a hydrophobic membrane module effectively captures oils from the emulsion, producing a dilute phase.[110,111] The integration of filtration and demulsification allows for the simultaneous recovery of both oil and water, achieving zero-liquid discharge; moreover, concentration adjustments within the system can enhance both processes, similar to the feedback in Janus channel of membranes. Throughout this operation, the feed alternates between hydrophilic and hydrophobic environments to facilitate the separation process. These findings present a novel perspective on the design of separation systems through the incorporation of Janus superiority spatially or temporally.

A Janus membrane enabling opposing processes on each side showcases the Janus superiority in reaction systems with synergistic effects. Elimelech’s group introduced a novel concept of a Janus electrocatalytic flow-through membrane, where one side functions as a cathode and the other as an anode.[112] Compared to conventional half-cell configurations, this design fully utilizes both cathodic reduction and anodic oxidation to generate singlet oxygen for water purification. Additionally, the flow-through mode, in which electrons flow parallel to the fluid direction, facilitates rapid charge transfer rates.

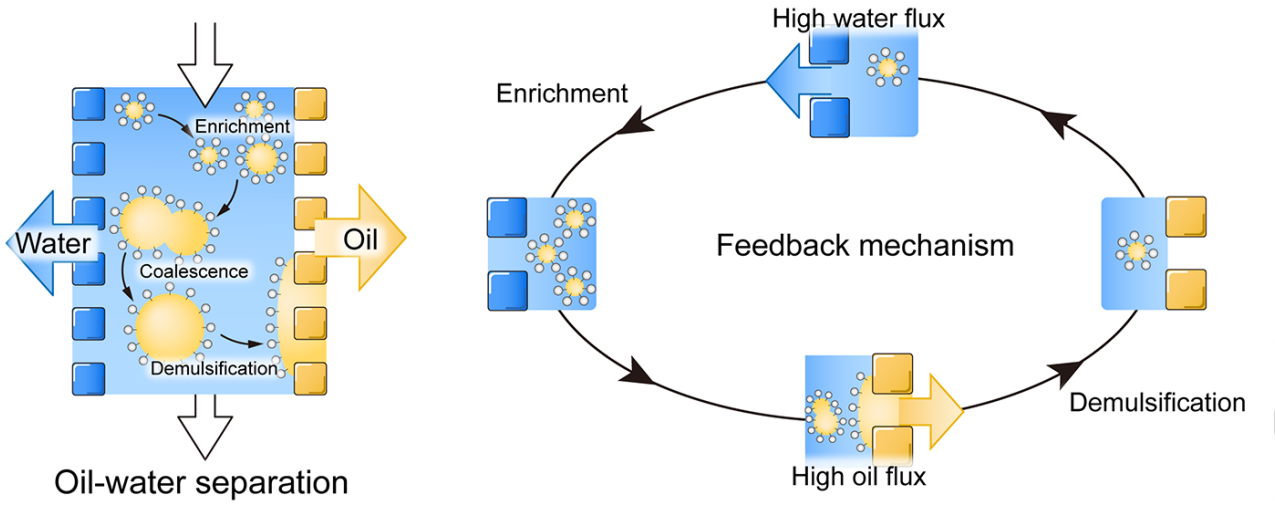

Figure 7. Mechanisms and feedback loop within the Janus channel of membranes for oil/water emulsion separation.

6. Future Perspectives

The concept of Janus superiority presents significant potential for advancing the design of membrane materials and separation systems across various scales, from nanoporous membranes to large-scale separation systems. Future research on fabrication methods is likely to focus on two key directions: precise fabrication techniques and scalability. Achieving precise microstructural control in Janus membranes requires further development of advanced manufacturing technologies, such as 3D printing, microfabrication, and area-selective ALD. Scaling up these technologies requires careful consideration of the specific property requirements for certain applications. For instance, biocompatibility is crucial for medical applications like wound dressings, while properties such as breathability and heat retention are vital for smart fabrics. In addition to the traditional considerations of opposing wettability and surface charges, future research could expand the scope of Janus configurations to include novel pairings, such as anode-cathode or donor-acceptor combinations, to further enhance the functionality of these materials.

From a process perspective, current research mainly investigates phase transfer and interphase molecular transport through Janus membranes, typically with pore sizes ranging from sub-microns to tens of microns. While the potential applications of Janus membranes in diverse scenarios are being actively explored, much of the current work focuses on phenomenological observations. A quantitative understanding of Janus superiority across different transport processes is still lacking. For instance, the upper performance limits of Janus membranes, especially when incorporating Janus configurations into homogeneous membranes, remain undefined both theoretically and experimentally. Machine learning offers powerful tools for identifying the key parameters influencing liquid transport and predicting membrane performance in specific applications. Although some studies have demonstrated electricity generation alongside mass transfer through Janus membranes, the mechanisms driving energy conversion—particularly the role of surface energy—are underexplored, with most research focusing on evaporation-driven processes. Future investigations are expected to address the water-energy nexus within Janus systems and their integration into device design. Additionally, incorporating directional fluid transport alongside subsequent reactions could further enhance the multifunctionality of Janus systems.

Emerging studies at both smaller and larger scales are broadening the applicability of Janus superiority and providing new directions for future research. The potential of nanoscale effects within Janus structures, which could enhance liquid-vapor transfer by increasing the driving force or reducing evaporation enthalpy at the microscale, remains largely unexplored. Furthermore, while membranes with hydrophilic and hydrophobic domains demonstrate excellent transport behavior for liquids of varying polarity, the role of Janus superiority in homogeneous molecular or ion transport, particularly in conventional Janus configurations with opposing wettability, has yet to be investigated. One particularly exciting prospect lies in the diode-like behavior exhibited by nanopore Janus membranes, which could have applications in nanofluidic neuromorphic computing[113,114]. Finally, Janus superiority in separation systems offers promising new approaches to device and process design. For example, Janus channels could integrate two mutually enhancing processes, overcoming the limitations of relying on a single process. This form of Janus superiority could be more readily implemented in practical applications, as it depends on the innovative design of devices and processes, rather than on material advancements alone.

Acknowledgements

Financial support for this work was provided by the National Natural Science Foundation of China (U21A20300) and Natural Science Foundation of Zhejiang Province (LZ25E030004). Work by SBD was supported as part of the Advanced Materials for Energy-Water Systems (AMEWS) Center, an Energy Frontier Research Center funded by the US Department of Energy, Office of Science, Basic Energy Sciences at Argonne National Laboratory under contract DE-AC02-06CH11357.

Keywords: Janus membrane • Phase transfer • Interphase transport • Directional transport

References

[1] D. S. Sholl, R. P. Lively, *Nature* **2016**, *532*, 435–437.

[2] B. E. Logan, M. Elimelech, *Nature* **2012**, *488*, 313–319.

[3] H. B. Park, J. Kamcev, L. M. Robeson, M. Elimelech, B. D. Freeman, *Science* **2017**, *356*, eaab0530.

[4] M. Elimelech, W. A. Phillip, *Science* **2011**, *333*, 712–717.

[5] H.-J. Huang, S. Ramaswamy, U. W. Tschirner, B. V Ramarao, *Sep. Purif. Technol.* **2008**, *62*, 1–21.

[6] H.-C. Yang, Y. Xie, J. Hou, A. K. Cheetham, V. Chen, S. B. Darling, *Adv. Mater.* **2018**, *30*, 1801495.

[7] J. Gu, P. Xiao, J. Chen, J. Zhang, Y. Huang, T. Chen, *ACS Appl. Mater. Interfaces* **2014**, *6*, 16204–16209.

[8] H. Wang, J. Ding, L. Dai, X. Wang, T. Lin, *J. Mater. Chem.* **2010**, *20*, 7938–7940.

[9] H.-C. Yang, J. Hou, V. Chen, Z.-K. Xu, *Angew. Chemie - Int. Ed.* **2016**, *55*, 13398–13407.

[10] P.-G. de Gennes, *Angew. Chemie Int. Ed.* **1992**, *31*, 842–845.

[11] H.-C. Yang, J. Hou, L.-S. Wan, V. Chen, Z.-K. Xu, *Adv. Mater. Interfaces* **2016**, *3*, 1500774.

[12] M. B. Wu, H. C. Yang, J. J. Wang, G. P. Wu, Z. K. Xu, *ACS Appl. Mater. Interfaces* **2017**, *9*, 5062–5066.

[13] Z. Wang, Y. Wang, G. Liu, *Angew. Chemie - Int. Ed.* **2016**, *55*, 1291–1294.

[14] F. Ren, G. Li, Z. Zhang, X. Zhang, H. Fan, C. Zhou, Y. Wang, Y. Zhang, C. Wang, K. Mu, Y. Su, D. Wu, *J. Mater. Chem. A* **2017**, *5*, 18403–18408.

[15] Y. Li, Z. Pei, D. Luan, X. W. D. Lou, *J. Am. Chem. Soc.* **2024**, *146*, 3343–3351.

[16] H. C. Yang, W. Zhong, J. Hou, V. Chen, Z. K. Xu, *J. Memb. Sci.* **2017**, *523*, 1–7.

[17] W. Xu, X. Hu, S. Zhuang, Y. Wang, X. Li, L. Zhou, S. Zhu, J. Zhu, *Adv. Energy Mater.* **2018**, *8*, 1702884.

[18] Y. Yang, X. Yang, L. Fu, M. Zou, A. Cao, Y. Du, Q. Yuan, C. H. Yan, *ACS Energy Lett.* **2018**, *3*, 1165–1171.

[19] Y. Cheng, J. Wang, X. Lu, C. Wang, *Nano Energy* **2023**, *117*, 108852.

[20] K. Li, H. N. Li, Y. R. Xue, H. C. Yang, C. Zhang, Z. K. Xu, *J. Colloid Interface Sci.* **2023**, *651*, 841–848.

[21] F. Bao, G. Pei, Z. Wu, H. Zhuang, Z. Zhang, Z. Huan, C. Wu, J. Chang, *Adv. Funct. Mater.* **2020**, *30*, 2005422.

[22] Z. Qiu, Y. Gao, D. Qi, M. Wu, Z. Mao, J. Wu, *Adv. Funct. Mater.* **2024**, *34*, 2311997.

[23] J. Gao, W. Guo, D. Feng, H. Wang, D. Zhao, L. Jiang, *J. Am. Chem. Soc.* **2014**, *136*, 12265–12272.

[24] J. C. Bui, E. W. Lees, D. H. Marin, T. N. Stovall, L. Chen, A. Kusoglu, A. C. Nielander, T. F. Jaramillo, S. W. Boettcher, A. T. Bell, A. Z. Weber, *Nat. Chem. Eng.* **2024**, *1*, 45–60.

[25] H.-J. Peng, D.-W. Wang, J.-Q. Huang, X.-B. Cheng, Z. Yuan, F. Wei, Q. Zhang, *Adv. Sci.* **2016**, *3*, 1500268.

[26] D. Chan, Y. Liu, Y. Fan, H. Wang, S. Chen, T. Hao, H. Li, Z. Bai, H. Shao, G. Xing, Y. Zhang, Y. Tang, *Energy Environ. Mater.* **2023**, *6*, e12451.

[27] L. Liu, H. Lan, Y. Cui, Q. Tang, J. Bai, X. An, M. Sun, H. Liu, J. Qu, *Sci. Adv.* **2024**, *10*, eadn8696.

[28] Z. Ai, Y. Zhao, L. Chen, T. Wen, S. Song, T. Zhang, *Sep. Purif. Technol.* **2022**, *300*, 121918.

[29] L. Hou, N. Wang, L. J. Yu, J. Liu, S. Zhang, Z. Cui, S. Li, H. Li, X. Liu, L. Jiang, Y. Zhao, *ACS Energy Lett.* **2023**, *8*, 553–564.

[30] Y. P. An, J. Yang, H. C. Yang, M. B. Wu, Z. K. Xu, *ACS Appl. Mater. Interfaces* **2018**, *10*, 9832–9840.

[31] H. Wang, H. Zhou, H. Niu, J. Zhang, Y. Du, T. Lin, *Adv. Mater. Interfaces* **2015**, *2*, 1400506.

[32] L. Hou, N. Wang, X. Man, Z. Cui, J. Wu, J. Liu, S. Li, Y. Gao, D. Li, L. Jiang, Y. Zhao, *ACS Nano* **2019**, *13*, 4124–4132.

[33] M. R. Jamalpour, A. Yadegari, F. Vahdatinia, L. M. Amirabad, S. Jamshidi, S. Shojaei, A. Shokri, E. Moeinifard, M. Omidi, L. Tayebi, *Dent. Mater* **2022**, *38*, 1316–1329.

[34] Z. X. Low, Y. T. Chua, B. M. Ray, D. Mattia, I. S. Metcalfe, D. A. Patterson, *J. Memb. Sci.* **2017**, *523*, 596–613.

[35] H. C. Yang, K. J. Liao, H. Huang, Q. Y. Wu, L. S. Wan, Z. K. Xu, *J. Mater. Chem. A* **2014**, *2*, 10225–10230.

[36] F. U. Ahmed, S. Sharma, D. D. Purkayastha, *ACS Appl. Mater. Interfaces* **2024**, *16*, 42641–42659.

[37] T.-D. Pan, Z.-J. Li, D.-H. Shou, W. Shou, J.-T. Fan, X. Liu, Y. Liu, *Adv. Mater. Interfaces* **2019**, *6*, 1901130.

[38] Z. Wang, X. Yang, Z. Cheng, Y. Liu, L. Shao, L. Jiang, *Mater. Horizons* **2017**, *4*, 701–708.

[39] X. Yang, L. Yan, F. Ran, A. Pal, J. Long, L. Shao, *J. Memb. Sci.* **2019**, *576*, 9–16.

[40] J. Chen, Y. Liu, D. Guo, M. Cao, L. Jiang, *Chem. Commun.* **2015**, *51*, 11872–11875.

[41] X. Tian, H. Jin, J. Sainio, R. H. A. Ras, O. Ikkala, *Adv. Funct. Mater.* **2014**, *24*, 6023–6028.

[42] Y. Cai, D. Chen, N. Li, Q. Xu, H. Li, J. He, J. Lu, *Sci. China Technol. Sci.* **2021**, *64*, 2211–2219.

[43] R. Z. Waldman, H. C. Yang, D. J. Mandia, P. F. Nealey, J. W. Elam, S. B. Darling, *Adv. Mater. Interfaces* **2018**, *5*, 1800658.

[44] A. He, C. Zhang, Y. Lv, Q. Z. Zhong, X. Yang, Z. K. Xu, *Macromol. Rapid Commun.* **2016**, *37*, 1460–1465.

[45] K. Sasaki, M. Tenjimbayashi, K. Manabe, S. Shiratori, *ACS Appl. Mater. Interfaces* **2016**, *8*, 651–659.

[46] J. Wang, Y. Zhou, L. Jiang, *Accounts Mater. Res.* **2023**, *4*, 86–100.

[47] K. Li, H. C. Yang, H. N. Li, C. Zhang, H. Q. Liang, Z. K. Xu, *Small Struct.* **2025**, *6*, 2400470.

[48] J. Wu, N. Wang, L. Wang, H. Dong, Y. Zhao, L. Jiang, *Soft Matter* **2012**, *8*, 5996–5999.

[49] W. Jia, J. A. Kharraz, J. Sun, A. K. An, *Desalination* **2021**, *520*, 115313.

[50] B. Mi, *Science* **2014**, *343*, 740–742.

[51] J. Lee, T. Laoui, R. Karnik, *Nat. Nanotechnol.* **2014**, *9*, 317–323.

[52] J. W. Elam, D. Routkevitch, P. P. Mardilovich, S. M. George, *Chem. Mater.* **2003**, *15*, 3507–3517.

[53] W.-Z. Fang, Y.-Q. Tang, C. Ban, Q. Kang, R. Qiao, W.-Q. Tao, *Chem. Eng. J.* **2019**, *378*, 122099.

[54] J. Wu, Z. Yan, Y. Yan, C. Li, J. Dai, *ACS Appl. Mater. Interfaces* **2022**, *14*, 49338–49351.

[55] W. A. Phillip, J. Rzayev, M. A. Hillmyer, E. L. Cussler, *J. Memb. Sci.* **2006**, *286*, 144–152.

[56] R. E. Beck, J. S. Schultz, *Science* **1970**, *170*, 1302–1305.

[57] Z. Ding, R. Ma, A. G. Fane, *Desalination* **2003**, *151*, 217–227.

[58] A. H. Persad, C. A. Ward, *Chem. Rev.* **2016**, *116*, 7727–7767.

[59] L. R. Fisher, R. A. Gamble, J. Middlehurst, *Nature* **1981**, *290*, 575–576.

[60] Q. Yang, P. Z. Sun, L. Fumagalli, Y. V. Stebunov, S. J. Haigh, Z. W. Zhou, I. V. Grigorieva, F. C. Wang, A. K. Geim, *Nature* **2020**, *588*, 250–253.

[61] J. M. Montes De Oca, J. Dhanasekaran, A. Córdoba, S. B. Darling, J. J. De Pablo, *ACS Nano* **2022**, *16*, 3768–3775.

[62] J. Yang, H. N. Li, Z. X. Chen, A. He, Q. Z. Zhong, Z. K. Xu, *J. Mater. Chem. A* **2019**, *7*, 7907–7917.

[63] Z. Wang, X. Wang, J. Xiong, M. Xie, Y. Shuai, *Chem. Eng. J.* **2024**, *498*, 155261.

[64] W. Zhang, L. Hu, H. Chen, S. Gao, X. Zhang, J. Jin, *J. Mater. Chem. B* **2017**, *5*, 4876–4882.

[65] B. Zhang, J. Li, J. Zhou, L. Chow, G. Zhao, Y. Huang, Z. Ma, Q. Zhang, Y. Yang, C. K. Yiu, J. Li, F. Chun, X. Huang, Y. Gao, P. Wu, S. Jia, H. Li, D. Li, Y. Liu, K. Yao, R. Shi, Z. Chen, B. L. Khoo, W. Yang, F. Wang, Z. Zheng, Z. Wang, X. Yu, *Nature* **2024**, *628*, 84–92.

[66] B. Xu, A. Li, R. Wang, J. Zhang, Y. Ding, D. Pan, Z. Shen, *Adv. Funct. Mater.* **2021**, *31*, 2105265.

[67] T. Yang, S. Wang, H. Yang, H. Gui, Y. Du, F. Liang, *Adv. Funct. Mater.* **2023**, *33*, 2214183.

[68] Z. Qiu, Y. Gao, D. Qi, M. Wu, Z. Mao, J. Wu, *Adv. Funct. Mater.* **2024**, *34*, 2311997.

[69] M. Xie, Z. Zhan, W. Xu, C. Zhang, Z. Wang, *Mater. Today Phys.* **2023**, *38*, 101246.

[70] H. C Zhang, Z. X Kang, Y. X Wu, Y. Pu, S. K Jiang, S. Amir, P. Wang, J. T Fan, *Nano Energy* **2024**, *128*, 109919.

[71] M. Zhao, Y. Liu, J. Zhang, H. Jiang, R. Chen, *J. Memb. Sci.* **2023**, *671*, 121418.

[72] Y. Chen, Z. Lu, Q. Liu, *J. Memb. Sci.* **2019**, *592*, 117384.

[73] C. Sun, R. Zhou, Z. Zhao, B. Bai, *J. Phys. Chem. Lett.* **2020**, *11*, 4678–4692.

[74] Y.-X. Huang, Z. Wang, J. Jin, S. Lin, *Environ. Sci. Technol.* **2017**, *51*, 13304–13310.

[75] J. Hou, C. Ji, G. Dong, B. Xiao, Y. Ye, V. Chen, *J. Mater. Chem. A* **2015**, *3*, 17032–17041.

[76] S. Gao, M. Mohammad, H. C. Yang, J. Xu, K. Liang, J. Hou, V. Chen, *ACS Appl. Mater. Interfaces* **2017**, *9*, 42806–42815.

[77] L. N. Rodrigues, K. K. Sirkar, K. R. Weisbrod, J. C. Ahern, U. Beuscher, *J. Memb. Sci.* **2021**, *637*, 119633.

[78] Z. Wang, X. Liu, J. Guo, T. A. Sherazi, S. Zhang, S. Li, *Chem. Commun.* **2019**, *55*, 14486–14489.

[79] N. G. P. Chew, Y. Zhang, K. Goh, J. S. Ho, R. Xu, R. Wang, *ACS Appl. Mater. Interfaces* **2019**, *11*, 25524–25534.

[80] Y. Chen, K.-J. Lu, S. Japip, T.-S. Chung, *Environ. Sci. Technol.* **2020**, *54*, 12713–12722.

[81] B. Nie, Y. Meng, S. Niu, L. Gong, Y. Chen, L. Guo, X. Li, Y.-C. Wu, H.-J. Li, W. Zhang, *Energy Environ. Sci.* **2025**, *18*, 3502–3525.

[82] H. N. Li, H. C. Yang, C. Y. Zhu, J. Wu, A. Greiner, Z. K. Xu, *J. Mater. Chem. A* **2022**, *10*, 20856–20865.

[83] X. Dong, H. Li, L. Gao, C. Chen, X. Shi, Y. Du, H. Deng, *Small* **2022**, *18*, 2107156.

[84] Y. Z. Chen, H. C. Yang, H. N. Li, J. H. Xin, C. Zhang, L. S. Wan, Z. K. Xu, *Small* **2024**, *20*, 2310952.

[85] Y. Dong, C. Violet, C. Sun, X. Li, Y. Sun, Q. Zheng, C. Tang, M. Elimelech, *Nat. Commun.* **2025**, *16*, 2659.

[86] B. Sun, M. Wu, X. Zhao, L. Wang, Y. Jia, Z. Yuan, H. Wu, J. Diao, G. He, X. Jiang, *Adv. Funct. Mater.* **2024**, *34*, 2406272.

[87] Y. Li, H. Chen, S. Xiao, M. A. Alibakhshi, C. W. Lo, M. C. Lu, C. Duan, *ACS Nano* **2019**, *13*, 3363–3372.

[88] Q. Xia, Y. Pan, B. Liu, X. Zhang, E. Li, T. Shen, S. Li, N. Xu, J. Ding, C. Wang, C. D. Vecitis, G. Gao, *Sci. Adv.* **2024**, *10*, eadj3760.

[89] J. H. Zhang, R. Mittapally, G. Lv, G. Chen, *Energy Environ. Sci.* **2025**, 1707–1721.

[90] G. Lv, Y. Tu, J. H. Zhang, G. Chen, *Proc. Natl. Acad. Sci.* **2024**, *121*, e2320844121.

[91] S. Zhao, C. Jiang, J. Fan, S. Hong, P. Mei, R. Yao, Y. Liu, S. Zhang, H. Li, H. Zhang, C. Sun, Z. Guo, P. Shao, Y. Zhu, J. Zhang, L. Guo, Y. Ma, J. Zhang, X. Feng, F. Wang, H. Wu, B. Wang, *Nat. Mater.* **2021**, *20*, 1551–1558.

[92] X. Sheng, Z. Liu, R. Zeng, L. Chen, X. Feng, L. Jiang, *J. Am. Chem. Soc.* **2017**, *139*, 12402–12405.

[93] S. Yan, Y. Li, X. Yang, X. Jia, J. Xu, H. Song, *Adv. Mater.* **2024**, *36*, 2307967.

[94] H. Huang, R. Shi, X. Zhang, J. Zhao, C. Su, T. Zhang, *Angew. Chemie - Int. Ed.* **2021**, *60*, 22963–22969.

[95] Y. Yang, W. Gao, Y. Chang, Z. Zhao, H. Shen, Z. Wang, T. Li, S. Zhao, *Cell Reports Phys. Sci.* **2023**, *4*, 101677.

[96] J. Liu, D. Hua, Y. Zhang, S. Japip, T. Chung, *Adv. Mater.* **2018**, *1705933*, 1705933.

[97] M. R. Puhan, P. Sarkar, R. Amal, G. Nagendraprasad, K. A. Reddy, B. Sutariya, S. Karan, *Adv. Mater.* **2024**, *36*, 2404164.

[98] M. Wu, Z. Li, Z. Yuan, H. Jiang, Y. Niu, X. Ruan, X. Yan, X. Li, X. Wu, G. He, X. Jiang, *Adv. Funct. Mater.* **2023**, *33*, 2210074.

[99] L.-J. Cheng, L. J. Guo, *Chem. Soc. Rev.* **2010**, *39*, 923–938.

[100] I. Vlassiouk, Z. S. Siwy, *Nano Lett.* **2007**, *7*, 552–556.

[101] Z. Zhang, X.-Y. Kong, K. Xiao, Q. Liu, G. Xie, P. Li, J. Ma, Y. Tian, L. Wen, L. Jiang, *J. Am. Chem. Soc.* **2015**, *137*, 14765–14772.

[102] X. Zhu, J. Hao, B. Bao, Y. Zhou, H. Zhang, J. Pang, Z. Jiang, L. Jiang, *Sci. Adv.* **2025**, *4*, eaau1665.

[103] W. Xin, L. Jiang, L. Wen, *Acc. Chem. Res.* **2021**, *54*, 4154–4165.

[104] J. Yang, P. Liu, X. He, J. Hou, Y. Feng, Z. Huang, L. Yu, L. Li, Z. Tang, *Angew. Chemie - Int. Ed.* **2020**, *59*, 6244–6248.

[105] S. Liu, C. Wu, W.-S. Hung, X. Lu, K.-R. Lee, *J. Mater. Chem. A* **2017**, *5*, 22988–22996.

[106] R. Zheng, S. Xu, S. Zhong, X. Tong, X. Yu, Y. Zhao, Y. Chen, *Environ. Sci. Technol.* **2024**, *58*, 22818–22828.

[107] X. Y. Guo, L. Zhao, H. N. Li, H. C. Yang, J. Wu, H. Q. Liang, C. Zhang, Z. K. Xu, *Science* **2024**, *386*, 654–659.

[108] B. E. Logan, M. Elimelech, *Nature* **2012**, *488*, 313–319.

[109] J. Ji, Q. Kang, Y. Zhou, Y. Feng, X. Chen, J. Yuan, W. Guo, Y. Wei, L. Jiang, *Adv. Funct. Mater.* **2017**, *27*, 1603623.

[110] L. Gou, M. Qiu, W. Ke, X. Chen, Y. Fan, *Sep. Purif. Technol.* **2024**, *334*, 126073.

[111] R. Zhu, H.-N. Li, X.-Y. Xia, X.-Y. Guo, X.-J. Huang, C. Zhang, H.-Q. Liang, H.-C. Yang, Z.-K. Xu, *Sep. Purif. Technol.* **2025**, *359*, 130552.

[112] Y. Zhao, M. Sun, X. Wang, C. Wang, D. Lu, W. Ma, S. A. Kube, J. Ma, M. Elimelech, *Nat. Commun.* **2020**, *11*, 6228.

[113] A. Noy, S. B. Darling, *Science* **2023**, *379*, 143–144.

[114] A. Noy, Z. Li, S. B. Darling, *Nano Today* **2023**, *53*, 102043.

Entry for the Table of Contents

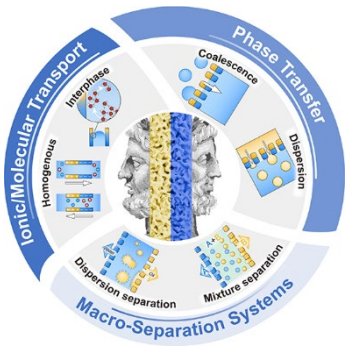

This review explores the Janus superiority of membrane materials in chemical engineering processes, with a focus on their design and fabrication principles, transport mechanisms, and diverse applications. It highlights their roles in chemical engineering and their multiscale impacts and concludes by discussing current challenges and future research directions.